Catheterization and Cardiovascular Interventions 65:288–294 (2005)

Basic Science Review

Real-Time Image Equalization for Coronary X-Ray Angiography

Normand Robert,[1]* PhD, Philip T. Komljenovic,[1] Stephen Fort,[2] MD, and J.A. Rowlands,[1] PhD

Coronary angiograms, which provide detailed images of contrast-filled coronary arteries, also show other large structures such as the diaphragm, spine and adjacent lung field. A real-time image processing method to attenuate these unwanted features is presented. Side-by-side comparisons of images selected from cine runs before and after processing show that the arteries in the processed images can be visualized more easily due to their higher contrast as other structures are made less prominent. It is also shown experimentally that this method allows more quantitative comparisons of the contrast of vessels in different parts of an image. © 2005 Wiley-Liss, Inc

INTRODUCTION

The primary aim of coronary angiography is the accurate visualization of contrast-filled blood vessels. X-ray signal intensity variations due to other structures such as the lungs, spine and diaphragm can stress the dynamic range of the detector and make the visualization of small blood vessels more difficult. The value of removing features in the images due to structures other than blood vessels was established with the development of digital subtraction angiography (DSA) [1]. However, DSA is not performed in coronary angiography owing to misregistration between the precontrast mask image and contrast-enhanced frames caused by cardiac and respiratory motions.

In coronary angiography, structures other than blood vessels are comparatively large in size. As a result, image equalization techniques that can attenuate large structures relative to smaller structures will result in images where blood vessels become more prominent. These techniques can be performed by introducing attenuators into the X-ray beam (X-ray equalization) and/or filtering the digitized images (postprocessing equalization).

A simple form of X-ray equalization (XRE) is commonly used in cardiac catheterization procedures through the introduction of a prepatient attenuating wedge into the field of view. The wedge is very effective at reducing brightening of the image due to the lungs if positioned with some care and panning is avoided during image acquisition. However, in some views, the wedge cannot be used to compensate for the dark shadows caused by the spine or diaphragm. To address these limitations, methods suitable for static imaging (radiography) have been proposed to modulate the input X-ray distribution spatially [2–4]. Adapting these methods for cine and fluoroscopy where images are acquired in rapid sequence in the presence of organ motion is difficult. Existing solutions produce a static attenuation pattern based on a single preexposure image, which cannot be changed dynamically during X-ray acquisition [5–7]. Postprocessing equalization, which can be done with software, does not require an elaborate mechanical system to equalize the dynamic X-ray attenuation distributions found in cardiac catheterization. Such techniques are an established approach used in many medical imaging applications to improve image display characteristics [8–10].

Some angiographic views result in images where differences in the attenuation of X-rays between various parts of the images are very large. If these differences exceed the dynamic range of the detector, parts of these images can-

[1]Department of Medical Biophysics, Imaging Research, Sunnybrook and Women's College Health Science Centre, University of Toronto, Toronto, Ontario, Canada
[2]Queen Elizabeth II Health Sciences Centre, Halifax, Nova Scotia, Canada

Grant support: the Canadian Institute for Health Research.

*Correspondence to: Normand Robert, Department of Medical Biophysics, Imaging Research, Sunnybrook and Women's College Health Science Centre, University of Toronto, 2075 Bayview Avenue, Room S633, Toronto, Ontario, M4N 3M5, Canada.
E-mail: robertn@cardioview.com

Received 3 May 2004; Revision accepted 18 January 2005

DOI 10.1002/ccd.20357
Published online 24 March 2005 in Wiley InterScience (www.interscience.wiley.com).

© 2005 Wiley-Liss, Inc.

not be recorded optimally. For example, a small feature of interest in a region of high X-ray transmission where the image is saturated, such as the lung, cannot be recovered through postprocessing alone. In these instances, a wedge can complement postprocessing equalization attenuating the bulk of the high transmission region so that postprocessing can complete the equalization.

We propose using a postprocessing equalization method that takes into account the X-ray attenuation process to remove signals due to structures other than blood vessels called self-masking subtraction angiography (SMSA). We previously applied this method to mask artifacts caused by a region of interest prepatient X-ray attenuator used to reduce the area exposure product in angiography [11]. The purpose of this investigation is to show that SMSA by itself is useful in conventional coronary angiography.

THEORY

The purpose of SMSA is to make the image intensity more uniform by reducing features in the image due to structures other than blood vessels. For each image in the sequence, SMSA requires computing a blurred version of the image, which is used as a mask to correct the original image. This procedure is performed on all images in a cine run. This postprocessing approach allows for real-time correction of images even as a patient or wedge moves or the detector is panned over the patient during X-ray acquisition.

Let us define I(u,v), the image recorded for each point (u,v) on the surface of the imaging detector (image intensifier or flat-panel). In the absence of scatter and beam hardening, the fractional transmission of X-rays through several overlapping structures equals the product of the transmission fractions of the individual layers as described by the Lambert-Beer law. Therefore, I can be separated into the product of the X-ray image due to the contrast-filled vessel V(u,v) and M(u,v), the X-ray image due to all other structures (lung, spine, muscle, etc.).

The vessel image V(u,v) is isolated by dividing the original image I(u,v) by M(u,v), the image due to all other structures. Thus, M acts as the mask image similar to that used in DSA. However, in coronary angiography, a frame acquired prior to contrast injection cannot be used as an estimate for M due to organ motion. Instead, it is proposed that an estimate for M denoted by $\tilde{M}$ be obtained by spatially blurring I(u,v) as described in the Appendix. Therefore, we write

$$\tilde{V}(u,v) = \frac{I(u,v)}{\tilde{M}(u,v)} \qquad (1)$$

We have chosen a Gaussian distribution as the blurring function because it attenuates higher spatial frequencies gradually (all of its derivatives are continuous). In X-ray imaging, greater spatial frequencies have a smaller signal-to-noise ratio and thus the application of such a filter results in a smooth image with reduced noise. The idea of using a blurred image to remove X-ray signals due to large structures has previously been applied to mammography [12] to reduce the X-ray signal in the peripheral portion of the breast where tissue thickness falls off rapidly.

Figure 1 describes the self-masking correction process on a simulated angiographic image. Figure 1a shows the attenuation caused by a contrast-filled vessel with a circular cross-section. Figure 1b shows the variation in X-ray attenuation due to a large structures exhibiting increased X-ray attenuation toward the bottom. Figure 1c illustrates the vessel in Figure 1a superimposed over the structures shown in Figure 1b. This profile was obtained by multiplying Figure 1a and b. This image represents the situation typically encountered in coronary angiography where a vessel overlaps another structure. Notice that the contrast of the vessel is no longer uniform from top to bottom. An estimate of the smooth background intensity variation $\tilde{M}$ is shown in Figure 1d and is based on a blurred version of the image in Figure 1c. It should be noted that this estimate of the background signal appears almost identical to the original background signal in Figure 1b apart from a slight shadow over the area corresponding to the vessel and thus constitutes a good mask image. Figure 1e shows the vessel following background correction using a method known as unsharp masking, where the estimate of the background intensity variation in Figure 1d is subtracted from Figure 1c. The contrast of the vessel is not constant over its length, making this approach undesirable. Figure 1f was obtained by taking the image in Figure 1c and dividing it by the estimate of the background intensity variation in Figure 1d. Notice that the vessel contrast is constant over the entire length of the vessel and nearly identical to Figure 1a, which only contains the signal due to the vessel.

For optimum results, the degree of blurring used to create the mask shown in Figure 1d must be chosen with some care. If $\tilde{M}$ is very blurred, the profile will have a constant value everywhere and application of our approach will have no effect on the images. If $\tilde{M}$ is insufficiently blurred, it will exhibit signal variations due to the vessel, resulting in a corrected image where the vessel will be altered. By blurring with a Gaussian function with the proper characteristic size (see Appendix), we have previously shown that the shape of vessel attenuation profile in the SMSA image is preserved in the final image and the signal-to-noise ratio is also maintained [11].

In this article, the effect of SMSA on a limited number of single frames from various cine runs is shown. Our approach was applied to every frame in each cine run. The filtering procedure has been optimized as described in the

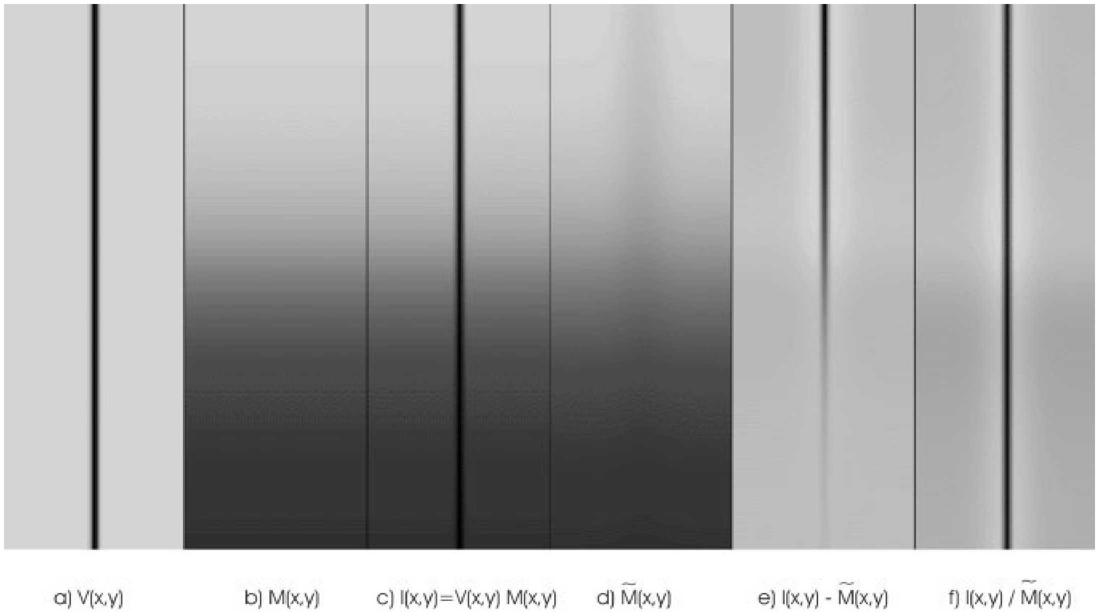

Fig. 1. The effect of a vessel and a background structure on a simulated angiographic image. a: The X-ray transmission due to the presence of a single vessel. b: The variation in X-ray attenuation due to a large overlying structures exhibiting increased X-ray attenuation toward the bottom. c: The superposition of the vessel on top of the structure in b as it would occur in an angiogram. d: A low-pass-filtered version of a to be used as an estimate for the mask image shown in b. e: An incorrectly restored image obtained by subtracting d from c. f: A correctly restored image obtained by dividing d into c. The vessel is nearly identical to that shown in a.

Appendix so that a single 512 × 512 pixel, 8 bit coronary angiographic frame could be equalized in 0.020 sec on a 2.53 GHz Pentium IV system (50 frame/sec).

METHOD

Clinical Images

SMSA was applied to various clinical images. An angiogram of a smaller patient, where wedge placement was good and the arteries were well opacified, was included to demonstrate that SMSA does not degrade good-quality images where vessels already exhibit good contrast. All the other images were selected because they were of poor quality due to large variations in attenuation, which made the simultaneous visualization of vessels in the over- and underexposed parts of the images difficult. This can occur because of poor wedge placement or inherent difficulties associated with image acquisition from certain angles exhibiting the spine and lung simultaneously. These views are sometimes needed to get an unobstructed view of a particular arterial segment.

For each case, the same image is shown before and after SMSA. In order to produce a fair comparison, both the conventional and SMSA images were rescaled in order to utilize the entire available gray-scale range. The images were acquired on a Philips cardiac X-ray image intensifier system and were recorded as a 512 × 512 pixel image sequence (8 bit depth) at 15 frames/sec with a 17 or 18 cm field of view. The resulting pixel size is 0.27 mm in the patient's heart, assuming a magnification of 1.25. The cine runs were recorded on DICOM format cardiology compact disks and were read with the aid of the Papyrus toolkit (University of Geneva).

X-Ray Phantom

To evaluate quantitatively how equalization reduces the effect of large background structures, X-ray images of a contrast-filled catheter simulating arteries were obtained. In this experiment, we examine how SMSA equalizes the vessel contrast over a region with varying attenuation due to background structures. Two contrast-filled 6 Fr catheters were placed on top of a two-step Lucite phantom. One catheter was placed on the thinner step having a thickness of 4.9 cm and the second catheter was placed on the thicker step having a thickness of 9.5 cm. Images of the phantom were acquired with our laboratory fluoroscopic system at 60 kVp, 2 mm Al filtration with an antiscatter grid.

Our system that performs quantitative coronary angiography measurements [13] was adapted to obtain estimates of the depth of the vessel (catheter) signal H as shown in Figure 2. The solid line in Figure 2 is the attenuation profile of a catheter obtained along a scan line perpendicular to the vessel centerline. The value of H is obtained from a least square fit of the vessel profile illustrated by the dashed line. As explained previously,

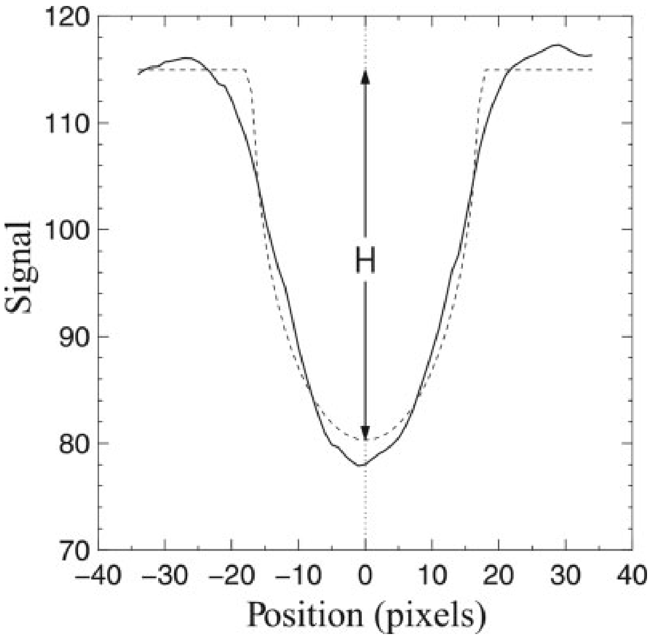

Fig. 2. Vessel profile obtained along a scan line perpendicular to the centerline of the vessel. The solid line illustrates the absorption of X-rays due a catheter. The dashed line is a least square fit of the catheter profile from which the vessel signal depth H is derived.

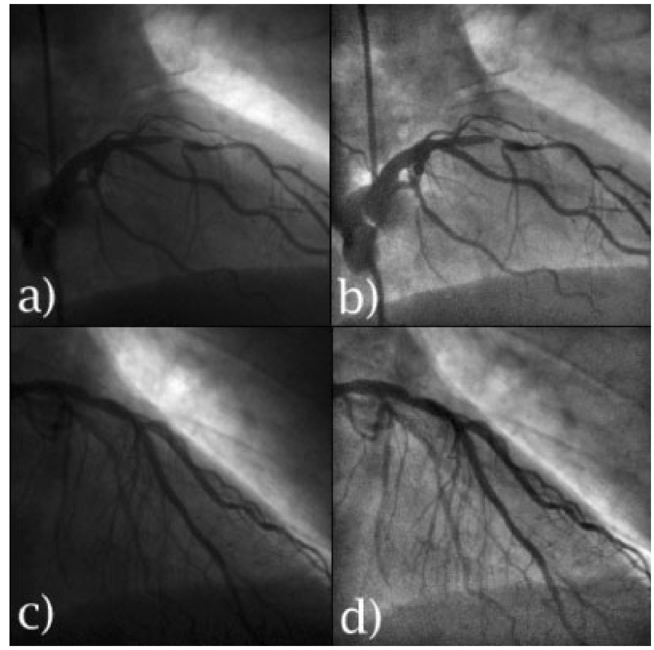

Fig. 3. The effect of equalization on images with poor wedge placement. a and c are the original RAO and RAO cranial image frames. b and d have been corrected using postprocessing (SMSA).

the value of H for a vessel not only depends on the amount of contrast in the vessel but also on the degree of X-ray absorption due to other overlapping structures. Thus, the catheter signal H_{thick} over the thick region of the phantom will be less than the catheter signal H_{thin} over the thin region of the phantom and H_{thin}/H_{thick} will be greater than 1. If the effect of background structures can be undone, a catheter will have an H value that is independent of background structures. Thus, in our phantom experiment, we expect H_{thin}/H_{thick} to have a value closer to 1 following equalization. This experiment demonstrates under realistic conditions how X-ray scatter, X-ray image intensifier veiling glare and beam hardening, can affect our ability to remove other structures.

RESULTS

Clinical Images

Figure 3a and c show two examples where wedge placement is suboptimal, causing a bright artifact near the edge of the silhouette of the heart. Figure 3b and d show how postprocessing equalization allows one to utilize more of the dynamic range of the display on the features of interest. When displaying images, only a finite number of gray levels are available. Some of the gray levels in Figure 3a are being wasted to display the brightened lung. More gray levels are available in the SMSA images to display arteries so they exhibit better contrast.

Figure 4a and c show two examples of diaphragms overlapping coronary arteries, thus darkening the arteries and impairing their visualization. Figure 4b and d show the same images following SMSA. The arteries overlapping the diaphragm can now be visualized more easily.

Figure 5 shows two such examples where equalization improves the visualization of the vessel over the thickest part of the mediastinum.

Figure 6 shows histograms of pixel values before and after SMSA computed from the images shown in Figure 5c and d. The vast majority of pixels in angiograms correspond to structures other than blood vessels, hence the histogram primarily captures the distribution of pixel values of these other structures. Prior to equalization, the histogram shows that these structures utilize a wide range of pixel values. After SMSA, these structures are confined to a narrower range of pixel values, making more gray levels available to display contrast-filled arteries.

Figure 7 illustrates an example of the application of SMSA on an image of good quality exhibiting a limited dynamic range, which is already optimal without postprocessing. Application of SMSA in this instance has almost no detrimental effect on the image as required.

X-Ray Phantom

Postprocessing equalization was performed on the images of the two contrast-filled catheters superimposed respectively on top of the thick and thin part of

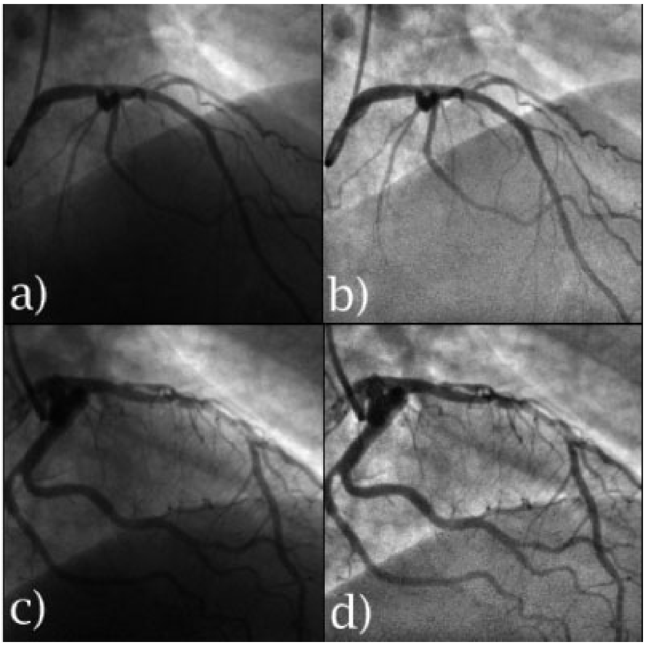

Fig. 4. The effect of equalization on images where vessels over the diaphragm have poor contrast. a and c are the original RAO cranial and RAO image frames. b and d are the SMSA images.

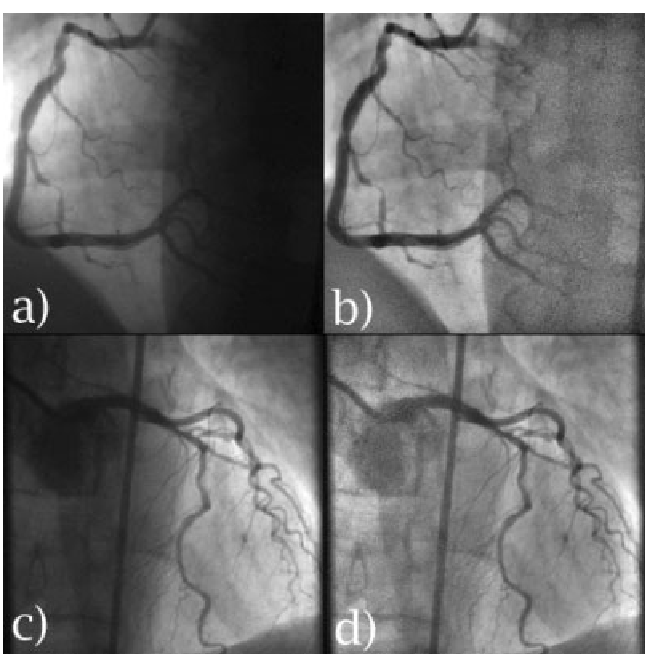

Fig. 5. The effect of equalization on images where the mediastinum and lung are in the field of view. a and c are the original LAO and AP cranial images. b and d are the corresponding SMSA images.

the phantom. The ratio of the catheter signal depth over the thin and thick parts of the phantom denoted by $H_{4.9\ cm}/H_{9.5\ cm}$ had a value of 2.90 ± 0.1. Following postprocessing equalization, this ratio was reduced

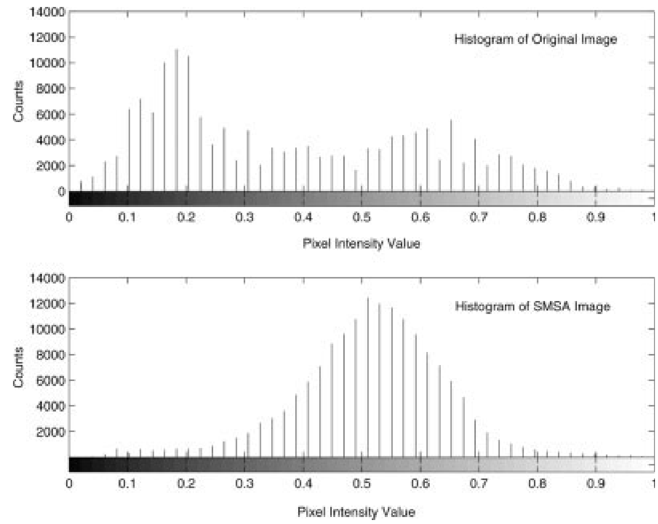

Fig. 6. Histograms showing the distribution of pixel values before (top) and after (bottom) SMSA.

to a value of 1.5 ± 0.1. The smaller H ratio following processing of the data is indicative of the reduced dependence of H on variations in attenuation due to background structures. Further improvement in our approach is possible by correcting for the effects of X-ray scatter [14,15] and beam hardening, which would result in an H ratio that is closer to 1. As a result, meaningful comparisons of the contrast of a vessel seen in different parts of an image can be made with greater confidence facilitating the assessment of eccentric en face lesions that have normal lumen boundaries but reduced contrast [16].

DISCUSSION

A simpler approach such as window and level manipulation of the image could have been used as an alternative to increase the number of display gray levels assigned to a particular vessel segment. However, this approach would prevent the simultaneous visualization of arteries in other parts of the image, where attenuation due to background structures is either greater or smaller. These arteries would respectively appear too dark or too bright. Reducing the contrast to see arteries in all parts of the image simultaneously would also reduce the contrast of the arteries. Thus, adjustments in window and level are inconvenient and require different settings for different parts of the image. These adjustments slow down the diagnostic process, making SMSA more advantageous.

In all the SMSA images, there is some overshoot/undershoot at the boundary of the diaphragm but none is noticeable over the edges of the arteries. X-ray noise is also more noticeable in parts of the images having a lower

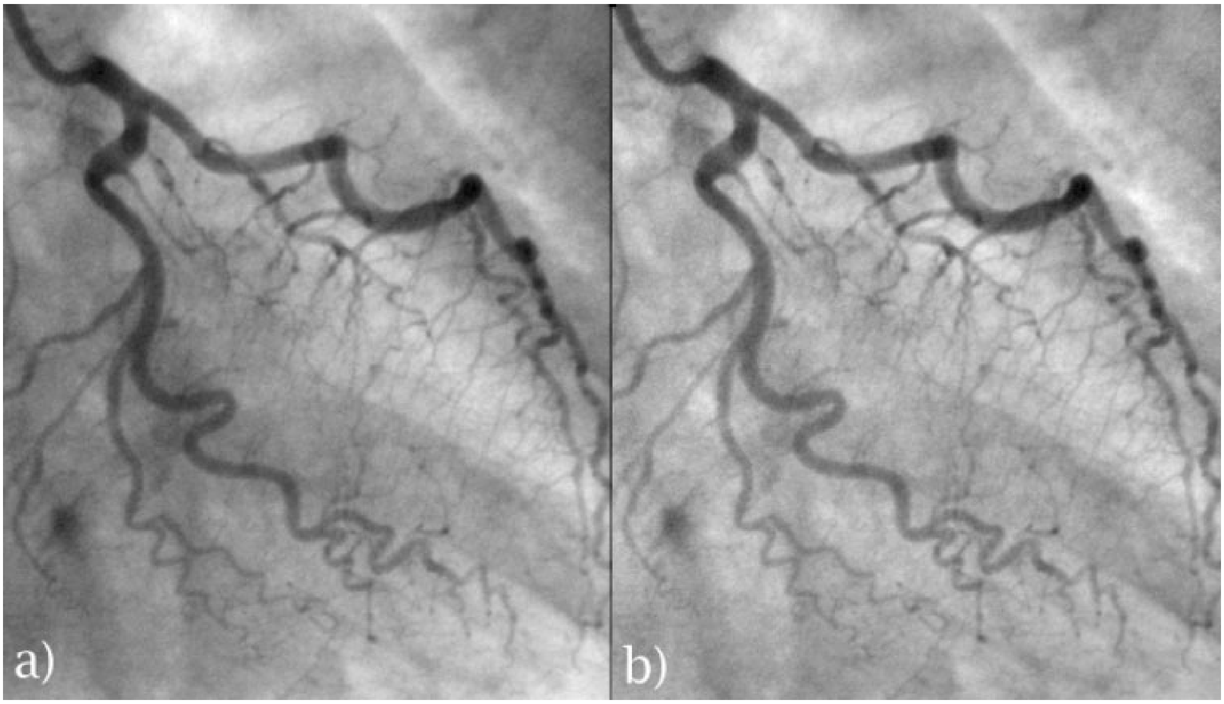

Fig. 7. The effect of equalization on an already uniform RAO caudal image. a: Original. b: SMSA.

exposure. This is not due to a decrease in signal-to-noise ratio relative to the conventional image. The mask image is computed at each point by combining pixel values over a neighborhood determined by the characteristic size of the Gaussian kernel. Thus, each point in the mask image is the result of the weighted average of approximately 200 pixel, making the noise in the blurred image negligible relative to the same point in the original image. Dividing each value in the original image by its corresponding nearly noise-free value in the blurred mask, as done in SMSA, rescales both the signal and the noise equally, maintaining the signal-to-noise ratio constant. The processed image is brighter in the low-exposure section so one can see the noise that was already present. If window and level adjustments were used to increase the contrast in the low-exposure region, the noise would become noticeable.

SMSA does conceal flush due to perfusion of the myocardium because it is a signal affecting a large area without sharp boundaries. In instances where a knowledge of perfusion is important, conventionally processed images should be examined as well.

The clinical images in this study are from an X-ray image intensifier system. Flat-panel-based catheterization systems have a greater dynamic range, reducing the need for the placement of wedges in order to obtain images of good quality over high- and low-exposure regions. Also, flat panels do not suffer from veiling glare, which reduces contrast [17]. SMSA-processed images can simultaneously render vessels over a wider range of X-ray exposures and thus image brightness. SMSA will be of benefit by allowing vessels in all parts of the image to be viewed with high contrast even with flat-panel-based systems. State-of-the-art X-ray angiography suites have the hardware capabilities to perform real-time image processing, including the method proposed here [18].

CONCLUSION

Coronary angiograms include structures other than blood vessels that stress the dynamic range of the detector and display systems. The angiographer can reduce but not eliminate this problem through careful positioning of the X-ray detector and the introduction of wedges. However, image quality is but one of the concerns that need to be addressed during catheterization and even experienced angiographers may occasionally acquire images that are suboptimal. SMSA is proposed as a method to attenuate signals due to structures other than blood vessels, allowing one to maximize the number of gray levels in the image used to display vessels. It was shown that SMSA is based on the physics of the interaction of X-rays, as is the case with DSA, which is not an option in coronary angiography due to organ motion. It was shown that this method reduces the variations in contrast of blood vessels between low- and high-exposure regions.

REFERENCES

1. Kruger RA, Mistretta CA, Crummy AB. Digital K-edge subtraction angiography. Radiology 1977;123:243–245.
2. Plewes DB, Vogelstein E. A scanning system for chest radiography with regional exposure control: practical implementation. Med Phys 1983;10:655–663.
3. Vlasbloem H, Kool LJ. AMBER: a scanning multiple-beam equalization system for chest radiography. Radiology 1988;169: 29–34.
4. Sabol JM. A scan-rotate geometry for efficient equalization mammography. Med Phys 1997;24:137.
5. Hasegawa BH, Dobbins JT, Naimuddin S, Peppler WW, Mistretta CA. Geometrical properties of a digital beam attenuator system. Med Phys 1987;14:314–321.
6. Boone JM, Gardiner GA, Levin DC. Filter wheel equalization in DSA: simulation results. Med Phys 1993;20:439–486.
7. Molloi S, Tang J, Mathur T, Zhou Y. Area X-ray beam equalization for digital angiography. Med Phys 1999;26:2684–2692.
8. Pisano ED, Cole EB, Major S. Radiologists' preferences for digital mammographic display. Radiology 2000;216:820–830.
9. Verellen D, De Neve W, Van den Heuvel F, Coghe M, Storme G. On-line portal imaging: image quality defining parameters for pelvic fields: a clinical evaluation. J Radiat Oncol Biol Phys 2000; 27:945–952.
10. Bankman IN. Handbook of medical imaging: processing and analysis. San Diego, CA: Academic Press; 2000. p 21–22.
11. Robert N, Komljenovic PT, Rowlands JA. A filtering method for signal equalization in region-of-interest fluoroscopy. Med Phys 2002;29:736–747.
12. Byng JW, Critten JP, Yaffe MJ. Thickness-equalization processing for mammographic images. Radiology 1997;204:564–568.
13. Robert N, Yaffe MJ, Langer A. Description and validation of a new quantitative coronary angiography system. Toronto: Annual Meeting of the Canadian Organization of Medical Physicists and the Canadian College of Physicists in Medicine; 1994.
14. Zhou YF, Mathurand T, Malloi S. Scatter and veiling glare estimation based on sampled primary intensity. Med Phys 1999;26:2301–2310.
15. Close RA, Shah KC, Whiting JS. Regularization method for scatter-glare correction in fluoroscopic images. Med Phys 1999; 26:1794–1801.
16. Thomas AC, Davies MJ, Dilly S, Dilly N. Potential errors in the estimation of coronary arterial stenosis from clinical arteriography with reference to the shape of the coronary arterial lumen. Br Heart J 1986;55:129–139.
17. Luhta R, Rowlands JA. Origins of flare in X-ray image intensifiers. Med Phys 1990;24:913–921.
18. Fajadet J, Marco J, Bertel O, Straumann E. Innovations in flat-detector cardiac angiography. Medicamundi 2003;47:56–60.

APPENDIX

The estimate of M(x,y) is obtained by blurring the original image I(x,y) computed by convolving the original image, I(x,y), with a blurring function K(x,y). In other words,

$$\tilde{M}(x,y) = I(x,y) ** K(x,y) \tag{2}$$

where $**$ is a two-dimensional convolution operator. The Gaussian symmetric two-dimensional distribution is defined as

$$K(x,y) = \frac{1}{2\pi\alpha^2} e^{-(x^2+y^2)/2\alpha^2} \tag{3}$$

where the parameter α, which characterizes the width of the function, is chosen so that smaller structures such as blood vessels are nearly completely blurred out of $\tilde{M}(x,y)$, simulating a precontrast image as obtained in DSA.

We have analyzed how the choice of α affects the shape of the vessel absorption profile and the signal-to-noise ratio of the image [11]. It was shown that for α values equal to the diameter of a blood vessel, the vessel cross-section was only slightly altered as the edges of the vessel were enhanced. In the case of α equal to or greater than twice the vessel diameter, the shape of the vessel profile is virtually unchanged. It was also shown that the signal-to-noise ratio of pixels in the SMSA image is nearly unchanged.

Choosing a value of α equal to the diameter of the largest vessel in the image results in the most aggressive equalization consistent with maintaining the shape of the vessel profile. We assume that the largest coronary arteries are 5 mm in diameter. Branch points are treated as vessels having double the diameter of the vessel segment upstream of the branch. Thus, we chose a blurring filter having an α value of 10 mm.

Multiple convolution operations with a box-shaped blurring function are equivalent to a single convolution operation with a Gaussian function by the central limit theorem. Convolution with a box function can be implemented to execute very quickly via sum tables, allowing SMSA to be performed at high frame rate using an all-purpose personal computer.

Some flat-panel systems can acquire images with $1{,}024 \times 1{,}024$ pixel $\times$ 12 bits at 30 frames/sec, increasing the amount of data to be processed 16-fold relative to the clinical images we have used. If required, the method can be sped up by subsampling the image, thereby reducing the number of pixels used in calculating the blurred mask. This can be achieved without degrading the SMSA image because the blurred mask is a weighted average of a large number of pixels and exhibits much less noise than the original image. Arteries that are the fastest moving structures found in angiograms are blurred out in the mask frames. Bulk patient motion, panning, and breathing are comparatively slow so large structures exhibit very little interframe motion. The absence of the fast-moving arteries in the mask images allows us to compute it for every second frame so that half the SMSA frames can use the mask image from the previous frame. Finally, if the SMSA images cannot quite be computed in real time, these images could still be shown more slowly in a first pass, stored and shown at full speed thereafter.